Received: 30 July 2020 | Revised: 20 September 2020 | Accepted: 7 October 2020

DOI: 10.1002/hbm.25250

RESEARCH ARTICLE

WILEY

Reference Ability Neural Network-selective functional connectivity across the lifespan

Georgette Argiris[1] | Yaakov Stern[1] | Christian Habeck[2]

[1]Cognitive Neuroscience Division, Columbia University, New York, New York

[2]Taub Institute, Columbia University, New York, New York

Correspondence
Christian Habeck, Columbia University Medical Center, Neurological Institute, 710 West 168th Street, 3rd floor, New York, NY 10032.
Email: ch629@cumc.columbia.edu

Abstract

Previous studies have demonstrated that four latent variables, or reference abilities (RAs), can account for the majority of age-related changes in cognition: these being episodic memory, fluid reasoning, speed of processing, and vocabulary. In the current study, we focused on RA-selective functional connectivity patterns that vary with both age and behavior. We analyzed fMRI data from 287 community-dwelling adults (20–80 years) on a battery of tests relating to the four RAs (three tests per RA = 12 tests). Functional connectivity values were calculated between a pre-defined set of 264 ROIs (nodes). Across all participants, we (a) identified connections (edges) that correlated with an RA-specific indicator variable and, indexing only these edges; (b) performed linear regression analysis per edge, regressing indicator correlations (Model 1) and connectivity values (Model 2) on Age, Behavioral Performance, and the Interaction term; and (c) took the conjunction of significant edges between models. Results revealed a different subset of edges for each RA whose connectivity strength and domain-selectivity varied with age and behavior. Strikingly, the fluid reasoning RA was particularly vulnerable to the effects of age and displayed the most extensive connectivity and selectivity "footprint" for behavior. These findings indicate that different functional networks are recruited across RA, with fluid reasoning displaying a special status among them.

KEYWORDS

cognition, cognitive aging, functional connectivity, reference ability neural networks

1 | INTRODUCTION

Several studies have reported a monotonic decline in cognitive abilities across the lifespan (see Salthouse, 2009a). Furthermore, the majority of age-related cognitive decline appears to be captured by four unique latent variables that have been derived based on a principle of shared variance across a variety of cognitive tests; termed "references abilities" (RAs), these are: episodic memory, fluid reasoning, speed of processing, and vocabulary (Salthouse, 2009b; Salthouse & Ferrer-Caja, 2003). While the utility of representing cognition in a comprehensive yet reductive manner has been largely acknowledged in the behavioral literature, fewer attempts have been made to map behavioral constructs onto their underlying neural substrates.

Previous work conducted in our lab successfully identified neural patterns uniquely associated with each of the four RAs (Habeck et al., 2016; Habeck, Eich, Razlighi, Gazes, & Stern, 2018; Stern et al., 2014). Participants had performed a series of in-scanner tasks related to each of the four RAs; voxel activations were then submitted to Principal Component Analysis to derive spatial covariance patterns across tasks related to the same domain. Interestingly, when these

reference ability neural networks (RANN) were derived in younger adults (<30 years) and predictive validity tested via out-of-sample classification performance, classification accuracy remained high even when testing on neural patterns derived in older adults. This finding suggested that there is a component to RANNs that is age-invariant and that RAs maintain their neural specificity across the lifespan (Habeck et al., 2016). In the current study, we attempted to extend previous findings demonstrating unique RANNs in the voxel activation data to functional connectivity collected from the same group of participants and as part of an ongoing study.

Advancing age has shown to be accompanied by altered functional networks, generally reflecting a decline in functional connectivity (see Liem, Geerligs, Damoiseaux, & Margulies, 2019, for a review). Recent studies have postulated age-related changes in functional network connectivity expressed as dedifferentiation— a reduction in specialized networks for specific cognitive processes (see Damoiseaux, 2017 for a review). For example, it is hypothesized that increasing age is associated with lower functional segregation, or a decrease in within-network connectivity compared to between-network connectivity, in distinct networks such as the default mode network (DMN; see Mak et al., 2017 for a meta-analysis). However, studies of task-related functional connectivity have evidenced both age-related increases and decreases in connectivity, particularly related to episodic and working memory, with the direction of age-related change potentially linked to performance and task difficulty (for a review, see Sala-Llonch, Bartrés-Faz, & Junqué, 2015). For example, Nagel and colleagues (2011) studied the effect of low versus high task load of an n-back task on blood-oxygen-level dependent (BOLD) activation in addition to functional coupling between task-relevant ROIs and a priori-defined seed region of the left dorsolateral prefrontal cortex (DLPFC). Older adults displayed a load-related increase in coupling between the DLPFC and the frontopolar and posterior temporal cortices but a decrease in connectivity between the DLPFC and premotor cortex. Other studies investigating episodic memory tasks have reported a reduction in functional connectivity between the hippocampus/medial temporal lobe and posterior and occipital regions while reporting an increase in connectivity between the hippocampus/medial temporal lobe and the PFC (Addis, Leclerc, Muscatell, & Kensinger, 2010; Dennis et al., 2008). These latter results have been interpreted as supporting a posterior–anterior shift with aging, which is a model based on voxel-based activation patterns that suggest an age-related reduction in occipital activity combined with increased functional activity (see Davis, Dennis, Daselaar, Fleck, & Cabeza, 2007); in this context, interpreting support for this model assumes that functional connectivity changes follow similar patterns as voxel activations (Sala-Llonch et al., 2015).

Few studies have investigated the relationship between functional connectivity and cognition as it relates to aging, and those that exist have largely been limited to episodic memory or processing speed, as it relates to DMN connectivity (Damoiseaux et al., 2008; Liem et al., 2019), whole-brain functional connectivity in episodic memory (Sala-Llonch et al., 2014), or resting-state changes as it compares to performance on neuropsychological tests (Onoda, Ishihara, & Yamaguchi, 2012). While this certainly does not comprise an exhaustive list, it does reflect gaps in the breadth of knowledge regarding age-related changes across multiple cognitive domains and their accompanying task-based functional correlates. Here, we analyzed the functional connectivity data collected from 287 participants with an age range between 20 and 80 years on a battery of tests comprising the four RAs considered to represent the breadth of age-related cognition. Exploiting an extensive battery of in-scanner testing, we were interested in identifying connections (i.e., edges) that commonly represented the tasks associated with each RA (e.g., domain-selective). A strength of our study design is that we test participants on multiple tasks that allow for analyses, such as within-domain task comparisons, that are performed on the same group of participants. Given the breadth of findings suggesting age-related changes in functional connectivity (Sala-Llonch et al., 2015) in addition to age-related changes across most cognitive domains (Salthouse & Davis, 2006), we were further interested in elucidating the effect of both age and behavior on domain-selectivity as well as strength of connectivity via linear regression analysis. In brief, our analytic approach first entailed deriving RA-selective edges based on linear indicator correlation. Next, using only those edges, we performed linear regression analysis, separately regressing the indicator correlation values and functional connectivity values on age, behavioral, and the interaction between the two. We then identified significant edges that overlapped between the terms of the two regression models. Given the novelty of studying the neural correlates related to the four latent RA, particularly their functional networks, we refrained from making strong a priori claims as to specific network configurations that might uniquely express age- or behavior-related changes. Instead, we merely expected that age-related differences would indeed manifest at the level of functional connectivity.

2 | METHODS

2.1 | Participants

Three hundred thirty-nine native English-speaking, right-handed (Oldfield Edinburgh Handedness Inventory; Oldfield, 1971) adults (age = 52.3 ± 16.71; range = 20–80 years) participated in the study. Participants were primarily recruited via random-market-mailing. All participants were screened for serious psychiatric or medical conditions, poor hearing and vision, and any other impediments that could hinder MRI acquisition; in addition, older participants were screened for dementia and mild cognitive impairment using the dementia rating scale (DRS; Mattis, 1988). Participants who then had more than 50% of their data "scrubbed," as explained in the *fMRI Data Preprocessing* section, were eliminated from the analysis. This procedure led to the removal of an additional 52 participants. Thus, 287 participants (154 females, 133 males) remained in the sample for analysis (age = 50.5 ± 16.92; range = 20–80 years), with a mean Nart IQ of 116.34 (± 8.92) and a mean education level of 16.28 (± 2.36) years. It is important to note that behavioral data were missing for some

participants due to software or hardware malfunction or incomplete task performance in certain cases. Thus, sample size varies depending on the task of analysis. Data counts are presented alongside the inferential statistics of our behavioral analyses.

2.2 | Procedure

FMRI data were acquired from participants as they performed 12 computerized cognitive tasks in-scanner, each relating to one of the four RAs (Stern et al., 2014). Participants completed the battery of tasks over two sessions, each lasting for ~2 hr and containing six of the 12 tasks belonging to two of the four RAs. Tasks within each reference domain were presented in a fixed order; however, the order of the two sessions was counterbalanced across participants. Prior to each scanning session, participants were familiarized with the six tasks relevant to the current session during an out-of-scanner training session, which was performed on a laptop computer. The mode of response for all but one task was keyboard button press; the picture-naming task used an oral response. Training sessions were self-paced such that breaks could be taken when needed and participants were given the option of repeating the training session if desired. In a separate session, participants also completed a neuropsychological battery; however, results from this battery will not be addressed in the current paper.

2.2.1 | Stimulus presentation

Stimuli were back-projected onto an LCD monitor positioned at the end of the scanner bore. Participants viewed the screen via a tilted mirror system that was mounted on the head coil. When needed, vision was corrected-to-normal using MR compatible glasses (manufactured by SafeVision, LLC. Webster Groves, MO). Responses were made on a LUMItouch response system (Photon Control Company). E-Prime v2.08, operating on PC platform, was used for stimulus delivery and data collection. Task onset was electronically synchronized with the MRI acquisition device.

2.2.2 | RA in-scanner tasks

Twelve cognitive tasks, each belonging to one of four reference domains, were presented in-scanner. A brief description of each task, divided by domain, is provided below (for a more thorough description, see Stern et al., 2014). For all tasks, except for picture naming, responses were made via button press; picture naming, instead, required a vocal response. For episodic memory, fluid reasoning, and vocabulary domains, accuracy—measured as the proportion of correct trials to total trials included—was analyzed for each task. For the processing speed domain, RT data were analyzed for each task. For the remainder of the document, an abbreviated version for each reference ability will be used: episodic memory—MEM, fluid reasoning—FLUID, processing speed—SPEED, and vocabulary—VOCAB. We also will interchangeably use the terms "domain" and "reference ability" to refer to our RAs.

Episodic memory

For all three episodic memory (MEM) tasks, both study and test phases were scanned together and cannot be separated in the analysis. The percentage of correct trials served as the behavioral variable of analysis.

Logical memory. Participants were presented with a story scenario on the computer screen. They were required to read the story and answer detailed multiple-choice questions regarding the content, choosing from four possible answers.

Word order recognition. In the study phase, participants were presented with a list of 12 words, one word at a time, on the computer screen and asked to remember the order of word presentation. In the test phase, participants were presented with a probe word at the top of the screen and four choice words below and asked to indicate which of the four choice words was presented subsequent to the probe word.

Paired associates. In the study phase, participants were presented with a list of 12 word-pairs, one pair at a time, on the computer screen and asked to remember the word pairings. In the test phase, participants were presented with a probe word and four choice words below and asked to select which word was previously paired with the probe word.

Fluid reasoning

The percentage of correct trials served as the behavioral variable of analysis (FLUID).

Matrix reasoning. Participants were presented with a matrix divided into nine cells (3×3), reflecting a particular pattern given by an unspecified rule, in which the bottom right cell though is empty. Eight figure choices were presented below the matrix and participants had to decide which figure best reflects the missing cell to complete the pattern (adapted from Raven 1962).

Letter sets. Participants were presented with five sets of letters where four out of the five letter sets expressed a common rule (e.g., contains no vowels). Participants were asked to infer the rule and identify the letter set that deviates from it (Ekstrom, Dermen, & Harman, 1976).

Paper folding. Participants were presented with a paper folded in a specific sequence with a set of holes punched through it. They had to decide which of six options, presented in two rows each containing three options, reflected the configuration of the holes on the paper when unfolded (Ekstrom et al., 1976).

Processing speed

Reaction time served as the behavioral variable of analysis (SPEED).

Digit symbol. Participants were presented with a code key at the top of the screen consisting of nine number (values ranging from one to nine)-symbol pairs. Below the code key a single number-symbol pair was presented and participants were asked to indicate if the pair was present in the code key (adapted from Salthouse, 1998).

Letter comparison. Participants were presented with two strings of letters, alongside one another, each containing three to five letters. They were asked to indicate whether the strings were the same or different (Salthouse & Babcock, 1991).

Pattern comparison. Participants were presented with two figures alongside one another, each containing lines that were connected in different configurations. They were asked to indicate whether the figures were the same or different (Salthouse & Babcock, 1991).

Vocabulary

The percentage of correct trials served as the behavioral variable of analysis (VOCAB).

Antonyms. Participants were presented with a probe word in capital letters at the top of the screen. Below the probe word, four choices of words were listed. They were asked to indicate which word possessed a meaning that was most *dissimilar* to that of the probe (Salthouse & Kersten, 1993).

Picture naming. Participants were presented with single images and asked to identify the picture by vocal response. Images were selected from the WJ-R Psycho-Educational battery (Salthouse, 1998; Woodcock, 1989).

Synonyms. Participants were presented with a probe word in capital letters at the top of the screen. Below the probe word, four choices of words were listed. They were asked to indicate which word possessed a meaning that was most *similar* to that of the probe (Salthouse & Kersten, 1993).

2.2.3 | fMRI data acquisition

Image acquisition was performed using a 3T Philips Achieva Magnet. There were two, 2-hr MR imaging sessions to accommodate the 12 fMRI activation tasks. At each session, a scout, T1-weighted image was acquired to determine participant position. Participants underwent a T1-weighted MPRAGE scan to determine brain structure, with a TE/TR of 3/6.5 ms and Flip Angle of 8°, in-plane resolution of 256 × 256, field of view of 25.4 × 25.4 cm, and 165–180 slices in axial direction with slice-thickness/gap of 1/0 mm. All scans used a 240 mm field of view. For the EPI acquisition, the parameters were: TE/TR (ms) 20/2000; Flip Angle 72°; In-plane resolution (voxels) 112 × 112; Slice thickness/gap (mm) 3/0; Slices 41. In addition, MPRAGE, FLAIR, DTI, ASL, and a 7-min resting BOLD scan were acquired. A neuroradiologist reviewed each participant's scans. Any significant findings were conveyed to the participant's primary care physician.

2.2.4 | fMRI data processing

Images were preprocessed using an in-house developed native space method (Razlighi et al., 2014). Briefly, the preprocessing pipeline included slice-timing correction and motion correction (MCFLIRT) performed using the FSL package (Jenkinson, Bannister, Brady, & Smith, 2002). All volumes were registered (6 *df*, 256 bins mutual information, and sinc interpolation) to the middle volume. Frame-wise displacement (FWD), as described in Power, Barnes, Snyder, Schlaggar, and Petersen (2012), was calculated from the six motion parameters and root-mean-square difference (RMSD) of the BOLD percentage signal in the consecutive volumes. To be conservative, the RMSD threshold was lowered to 0.3% from the suggested 0.5%. Contaminated volumes were then detected by the criteria FWD > 0.5 mm or RMSD >0.3% and replaced with new volumes generated by linear interpolation of adjacent volumes. Volume replacement was performed before temporal filtering (Carp, 2013). Flsmaths–bptf (Jenkinson et al., 2002) was used to pass motion-corrected signals through a bandpass filter with cut-off frequencies of 0.01 and 0.09 Hz. Finally, the processed data were residualized by regressing out the FWD, RMSD, left and right hemisphere white matter, and lateral ventricular signals (Birn, Diamond, Smith, & Bandettini, 2006).

2.2.5 | Functional connectivity

T1 image segmentation was performed using FreeSurfer (Dale, Fischl, & Sereno, 1999). The coordinates of 264 putative functional nodes derived from a network partition scheme developed by Power et al. (2011) were transferred to each participant's T1 space via nonlinear registration of the participant's structural scan to the MNI template using the ANTS software package. Next, a 10 mm radius spherical mask, centered at each transferred coordinate, was generated and intersected with the FreeSurfer gray matter mask in order to obtain the ROI mask for the 264 functional nodes. An intermodal, intra-subject, rigid-body registration of fMRI reference image and T1 scan was performed with FLIRT with 6 degrees of freedom, normalized mutual information as the cost function (Jenkinson & Smith, 2001), and used to transfer all ROI masks from T1 space to fMRI space. These transferred ROI masks were then used to average all the voxels within each mask to obtain a single fMRI time-series for each node. Pearson correlations were then performed for all pairwise combinations. This resulted in 264 x 263/2 = 34,716 functional connectivity pairs, or *edges*.

Given the differing nature of the task, the length of the time-series varied for each. The following represents the number of TRs

(1 TR = 2000 ms) per task: MEM: Log_Mem—210, Word_Order—208, Pair_Assoc—99; FLUID: Mat_Reason—430, Letter_Sets—430, Paper_Fold—430; SPEED: Digit_Sym—210, Letter_Comp—195, Pattern_Comp—190; VOCAB: Antonyms—194, Pic_Name—190, Synonyms—194.

2.3 | Analytical approach

Data were analyzed and brain connectivity graphs created using custom-written MATLAB® codes (Mathworks, Natick, MA). Brain maps were generated using BrainNet Viewer (Xia, Wang, & He, 2013). FC correlation values (*r*) between nodes were converted to *Z* coefficients using Fisher's transformation (i.e., inverse tangent of *r*). In order to standardize comparisons between tasks, behavioral scores were z-transformed using the mean and *SD* calculated across all participants for each task separately. Given that speed tasks were measured as reaction time, z-score values were sign-inverted to correspond with accuracy scores, whereby higher scores always indicate better performance. Age effects were tested using age as a continuous factor in regression analyses. For regression models, behavior and age factors were mean-centered to remove any potential interferences of multicollinearity (Aiken & West, 1991). Furthermore, operating under the assumption of within-domain task similarity, functional connectivity values were averaged across tasks within each domain, rendering a reduced matrix of 34,716 edges × 287 subjects × 4 domains. To demonstrate that this was an analytically sound approach, we employed a simple out-of-sample classification procedure using permutation analysis. We divided the data into training (215 participants, or 75% of the sample) and testing (72 participants, or 25% of the sample) sets, computing the mean within-domain map across the three tasks and participants in the training set for each of the four domains, which served as reference "dictionary" by which to compare our test sample. We then classified all held-out data at the individual level by correlating each individual's task vector (=12) with the dictionary. For each task, the winning "vote" was assigned to the domain that displayed the highest Pearson's R correlation. This procedure was repeated 1,000 times by permuting training/testing set assignment across iterations, generating different set combinations. We then obtained accuracy scores by summing across all 1,000 iterations and dividing by the number of permutations, per task and individual, and then averaging across individuals. This rendered a 12 × 4 matrix of accuracy scores for each task across domains. Our results showed that tasks were correctly classified according to their domain well above chance level (25% chance) for all 12 tasks (see Figure S1 and Table S1).

2.3.1 | Indicator variable correlation (RA domain-selectivity)

To obtain connectivity edges that were selective to each RA domain, an indicator variable, or binary vector, was used to correlate with the FC *Z*-coefficients across tasks for each connectivity pair. We used indicator correlation to identify the edges that express *similarity* in their FC values based on RA domain, such that those edges highly selective for a particular RA will correlate highly with the vector expressing the domain of interest. In this way, selectivity will be expressed as the relation between the FC values and the vector pattern. For instance, to detect memory-selective edges among connectivity edges (c = 1…34,716), we created the 12 × 1 vector as:

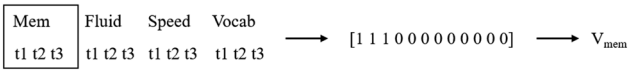

We then correlated this vector with the 12 × 1 FC values for each edge (c) and converted the resulting *r* coefficient to *Z*, thus yielding a single correlation value $Z(c)_{mem}$ for each of the 34,716 connectivity edges. This correlation was performed for each RA domain (d = 1…4) at the single-participant level (s = 1…287), such that

$$\operatorname{arctanh}\left(\operatorname{Corr}\left(V_{mem}, FC_{(c,s)}\right)\right) = Z(c,s)_{mem}$$

where V_{mem} is the indicator vector for memory expressed above, $FC_{(c, s)}$ is the 12 task FC values for a given edge (c) and subject (s), and $Z(c, s)_{mem}$ is the resulting single *Z*-coefficient after Fisher's (arctanh) transformation. This process was repeated four times, each time correlating the same 12 × 1 $FC_{(c, s)}$ vector with the indicator vector corresponding to one of the four domains. Whereas in the example above, the indicator vector for memory is expressed as [111000000000], for fluid reasoning it would be expressed as [000111000000], for processing speed it would be expressed as [000000111000], and for vocabulary it would be expressed as [000000000111]. The final result was a third-rank matrix *Z*(c, s, d) with format [Z] = 34,716 × 287 × 4 of indicator correlation values.

In order to establish significant edges, multiple one-way *t*-tests against chance were performed across participants on this third-rank [Z] matrix, for each pair (c) and domain (d). This process resulted in a matrix of *t*-values– *t*(c, d), and corresponding *p*-values– *p*(c, d). As *t*-values could reflect a relationship in either the positive or negative direction, we divided edges by the sign of their *t*-values, which indicated positive versus negative correlations between the FC values and indicator vector. We chose an uncorrected *p*-value significance threshold of .001 and selected only those edges falling below this cutoff. For the purposes of the present analyses, only edges with a positive *t*-statistic were considered beyond this point for further analyses, as we were interested in those edges that demonstrated a positive relationship between FC values and cognitive domain. We refer to these edges as domain-selective.

2.3.2 | Regression models with RA-selective edges

For each RA domain, we indexed the domain-selective edges resulting from the one-way *t*-test analyses and performed multiple linear regression on each of these edges. We considered the effect of *Age*,

Behavioral Performance, and their *Interaction* on both (a) the FC values and (b) the strength of domain-selectivity, across individuals. Including the interaction term in our models allowed us to test for a possible moderating effect of *Age* on the strength of the relationship between brain and behavior. All predictor terms were simultaneously included in the model, creating the full model, separately, for both connectivity values and domain-selectivity values, rather than generating multiple models by including one predictor variable at a time in a stepwise fashion. Ultimately, we were interested in elucidating the effect of the predictor variables on both domain-selectivity and the connectivity values themselves.

Indicator correlation regression model

For each domain, we returned to the [Z] matrix of indicator correlation values and selected the subarray of edges that expressed domain-selectivity, resulting in a reduced matrix $Z(c_{select}, s, d)$, where (c_{select} = 1…number of domain-selective edges per domain; s = 1…287; d = 1…4). Next, for each edge of each domain, we created a full linear regression model, regressing the indicator correlation *Z*-coefficients *Z*(s = 1…287) across all participants on Age, Behavioral Performance, and the Interaction (Age × Behavior), exemplified as

$$\text{Significant } \Delta \text{ selectivity}_{(\text{domain})} = Z(c_{select}, d) \sim \text{Age} + \text{Behavior} + \text{Age} * \text{Behavior}$$

where for each predictor term (=3 in total), we selected those edges that demonstrated a significant effect on the indicator correlation values at a *p*-threshold of .001, uncorrected.

Functional connectivity values regression model

Identical to the indicator correlation regression model, for each domain, we again selected the subarray of edges that expressed domain-selectivity, only this time to return to their corresponding FC connectivity values. We refer to this matrix as $ConnZ(c_{select}, s, d)$. As before, per edge of each domain, we created the full linear regression model, regressing the participant-level connectivity correlation *Z*-coefficients ConnZ(s = 1…287) on Age, Behavioral Performance, and the Interaction (Age x Behavior), exemplified as

$$\text{Significant } \Delta \text{ connectivity}_{(\text{domain})} = ConnZ(c_{select}, d) \sim \text{Age} + \text{Behavior} + \text{Age} * \text{Behavior}$$

where for each predictor term, we again selected those edges that demonstrated a significant effect on the connectivity values at the *p*-threshold of .001, uncorrected.

Significant edge overlap between models

After establishing the edges whose variation in indicator and FC correlation values was separately and significantly predicted by age, behavioral performance, or the Interaction, we examined the edge overlap emerging from both indicator and FC correlation regression analyses. That is, for each predictor term (3) in each domain (4), we determined which edges were significant in both regression models. For instance, we tallied edges whose domain-selectivity to memory and FC-strength in the memory tasks both showed significant associations with memory performance.

2.3.3 | Statistical analysis

For testing age effects on behavioral task performance, linear regression analysis was used. False Discovery Rate (FDR) as described by Benjamini and Yekutieli (2001) was used to control for multiple comparisons (i.e., 12 comparisons). A result was considered significant if its corresponding p-value was below the critical p-value calculated to control for false positives at the standard rate of <5% (q = 0.05). Conversely, for regression models built on the neural data, the established threshold for significance across all analyses was $p < .001$, uncorrected.

3 | RESULTS

3.1 | Behavioral

We first report the findings from the effects of age on behavioral performance. Regression analysis revealed a significant effect of Age on Behavioral Performance (critical $p < .0048$; Benjamini-Yekutieli corrected) on most neuropsychological tests. The only task in which performance was not significantly related to age was for Logical Memory of the MEM domain. Otherwise, age was negatively related to performance, meaning that increasing age was linked to reduced performance on tasks of memory, fluid reasoning, and processing speed. Conversely, on all three vocabulary tasks, age was positively related to performance, meaning that participants' performance improved with increasing age. These findings were generally in line with previous studies (Salthouse & Davis, 2006; Stern et al., 2014). Inferential statistics of task performance including the number of participants for whom behavioral data was available for analysis can be found in Table 1. Discrepancies in data counts were attributable to software or hardware malfunction or incomplete task performance in certain cases.

3.2 | Indicator variable correlation (RA domain-selectivity)

One-way *t*-tests across participants revealed several edges that were RA-selective (see Table 2 for significant edge counts). As a reminder, only edges demonstrating a positive relationship between the indicator vector and within-domain connectivity values are considered domain-selective and reported. Overall, the number of MEM-selective positive edges was higher than edge-selectivity for any other domain. This was followed by the FLUID domain, then SPEED, and finally VOCAB.

TABLE 1 Inferential statistics for the linear regression model performance∼age

Task	Domain		Age predictor			
		N	*B*	*t*	*p*	p_{adj}
Log_Mem	MEM	253	−0.009	−2.35	.02	ns
Word_Order	MEM	255	−0.021	−5.94	<.001	**<.001**
Pair_Assoc	MEM	251	−0.016	−4.53	<.001	**.001**
Mat_Reason	FLUID	257	−0.020	−5.75	<.001	**<.001**
Letter_Sets	FLUID	258	−0.010	−2.84	.005	**.016**
Paper_Fold	FLUID	250	−0.020	−5.62	<.001	**<.001**
Digit_Sym	SPEED	268	−0.035	−11.60	<.001	**<.001**
Letter_Comp	SPEED	270	−0.026	−7.85	<.001	**<.001**
Pattern_Comp	SPEED	274	−0.023	−6.78	<.001	**<.001**
Antonyms	VOCAB	271	0.014	3.98	<.001	**.001**
Pic_Name	VOCAB	262	0.023	6.74	<.001	**<.001**
Synonyms	VOCAB	263	0.020	5.61	<.001	**<.001**

Note: Tasks displaying a significant effect of age on behavioral performance is presented in bold face. Abbreviations: *B*, standardized Beta coefficient; N, number of people for whom data were present; ns, nonsignificant; *p*, unadjusted *p*-value; p_{adj}, adjusted *p*-value from Benjamini-Yeku; *t*, t-statistic.

TABLE 2 Number of significant edges per domain

Domain	Indicator selectivity	Regression with indicator correlation as outcome			Regression with functional connectivity as outcome			Overlap of both regression		
	Positive	Age	Beh	Inter	Age	Beh	Inter	Age	Beh	Inter
MEM	3,918	**46**/44	**5**/0	**3**/3	**44**/7	**6**/1	**7**/1	**0**	**1**/0	**0**
FLUID	3,820	**14**/10	**107**/0	**2**/1	**343**/298	**95**/0	**1**/1	**6**/5	**32**/0	**0**
SPEED	3,238	**40**/14	**11**/9	**1**/0	**254**/142	**7**/7	**3**/1	**31**/9	**2**/2	**1**/0
VOCAB	2,403	**13**/13	**1**/0	**5**/2	**58**/42	**3**/0	**5**/1	**3**/3	**1**/0	**1**/0

Note: Number of significant edges per domain (column 1) from (a) Indicator correlation domain-selectivity analysis (column 2); (b) Indicator correlation regression (columns 3–5); (c) Connectivity correlation regression models (columns 6–8); and the (d) Overlap of significant edges between indicator and connectivity regression models, per predictor term (Age, Behavior, and the Interaction) (columns 9–11). The bolded number on the left represents the total number of significant edges while the number on the right represents the number of significant edges displaying a negative relationship between the predictor term and outcome variable.

To see whether the majority of participants truly expressed domain-selective edge selectivity, we averaged across the original *Z*-coefficients of significant edges in each domain for each of the 12 tasks at the participant-level. For instance, for those edges that expressed MEM-selectivity, we indexed the original *Z*-coefficients pertaining to those edges, not for memory tasks alone but for all 12 tasks in order to observe the strength of connectivity expressed in those edges in all domains. We then calculated the average across those edges for each task, for each participant, repeating this process for the significant edges from each domain. For graphs of the average correlational values across edges per participant, see Figure 1. As can be observed from the figure, for all domains, edges that expressed selectivity for a particular domain consistently demonstrated higher FC coefficients in tasks that related to that domain in the majority of participants. It is important to note that while edge RA-selectivity was not necessarily unique to a given RA, any nonunique overlap is likely due to different participants driving an edge's selectivity. We tested this speculation by correlating the indicator correlation values, obtained at the individual participant level, for one domain with those of the other for all edges that expressed edge overlap. That is, for each domain combination (6 in total: MEM-FLUID: 324 edges; MEM-SPEED: 39 edges; MEM-VOCAB: 632 edges; FLUID-SPEED: 558 edges; FLUID-VOCAB: 30 edges; SPEED-VOCAB: 187 edges), for each overlapping edge, we returned to the original [Z] indicator correlation matrix (34,716 edges × 287 participants × 4 domains) and selected the two across-participant vectors of indicator correlation values corresponding to an edge of overlap for a given domain combination. The assumption was that across-participant correlation should be either low or negative between two domains' indicator correlation values if different participants are driving selectivity in each domain. We indeed found this to be the case with all but two edges displaying negative correlation. We randomly selected an overlapping edge from each domain combination and graphically present each participant's indicator correlation values linked between domains in Figure S2.

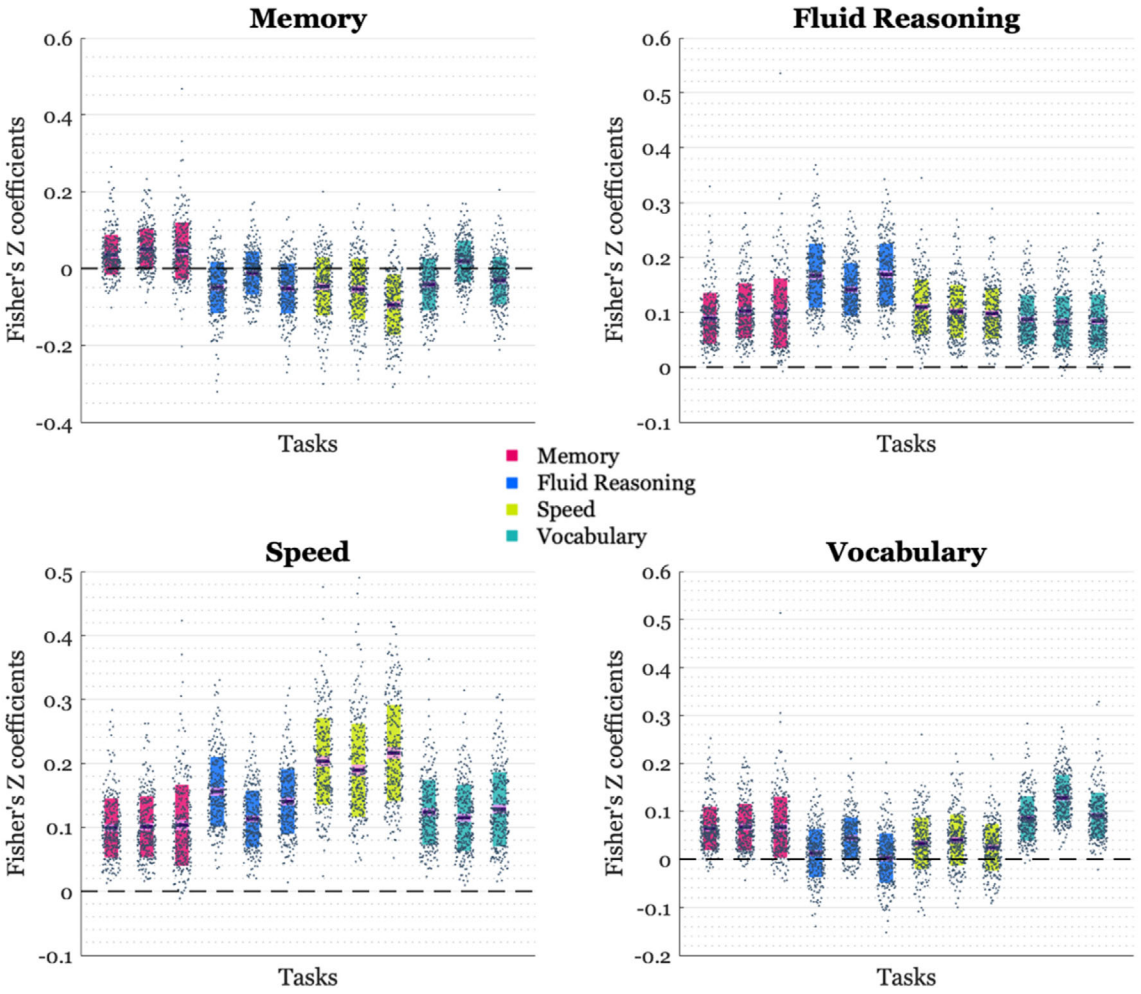

FIGURE 1 Scatterplots of functional connectivity Fisher's Z coefficients averaged across all edges demonstrating RA domain selectivity in each domain, per participant (dots), for each of the 12 tasks; selectivity is defined as those edges significantly positively correlated with the indicator variable. For example, for the "Memory" plot, the Fisher's Z-coefficients relating to only significant Memory edges were averaged within each participant for each of the 12 tasks, such that average connectivity values should be higher in memory tasks than for any of the other tasks. As can be observed from the plots, this was generally the case. The color of each box corresponds to domain of the task, the expanse of the box represents one *SD*, the pink middle strip represents the *SEM* for the 95% confidence interval, and the purple line represents the mean

3.3 | Regression models

3.3.1 | Associations of domain-selectivity regression

Age

For each domain, we again indexed domain-selective edges and performed regression analysis per edge, regressing the participant-level indicator correlations on Age, Behavior, and the Interaction term. There was a generally negative relationship between age and the indicator correlation values, except for the SPEED domain, which demonstrated a mainly positive relationship, specifically in bilateral posterior cortical regions, with few negative long-range connections extending mainly from left anterior regions to bilateral posterior regions (see left section of Figure 2). In addition, one node in the right superior posterior cortex (medial temporal lobe) served as a connective "hub." Not only did this node display a positive relationship between age and domain-selectivity, but a negative relationship between behavior and domain-selectivity; that is, as domain-selectivity increased with age, behavioral performance decreased.

Conversely, the MEM domain primarily possessed several connections displaying a negative relationship between age and domain-selectivity at posterior cortical sites, with a slightly right hemispheric bias.

Behavior

When considering behavior after controlling for age, significant edges mainly displayed a positive relationship between behavior and domain-selectivity—that is, as domain-selectivity was increasing, behavior was also increasing (see left section of Figure 3). However, the SPEED domain mainly displayed edges with a negative relationship between domain-selectivity and behavioral performance. Interestingly,

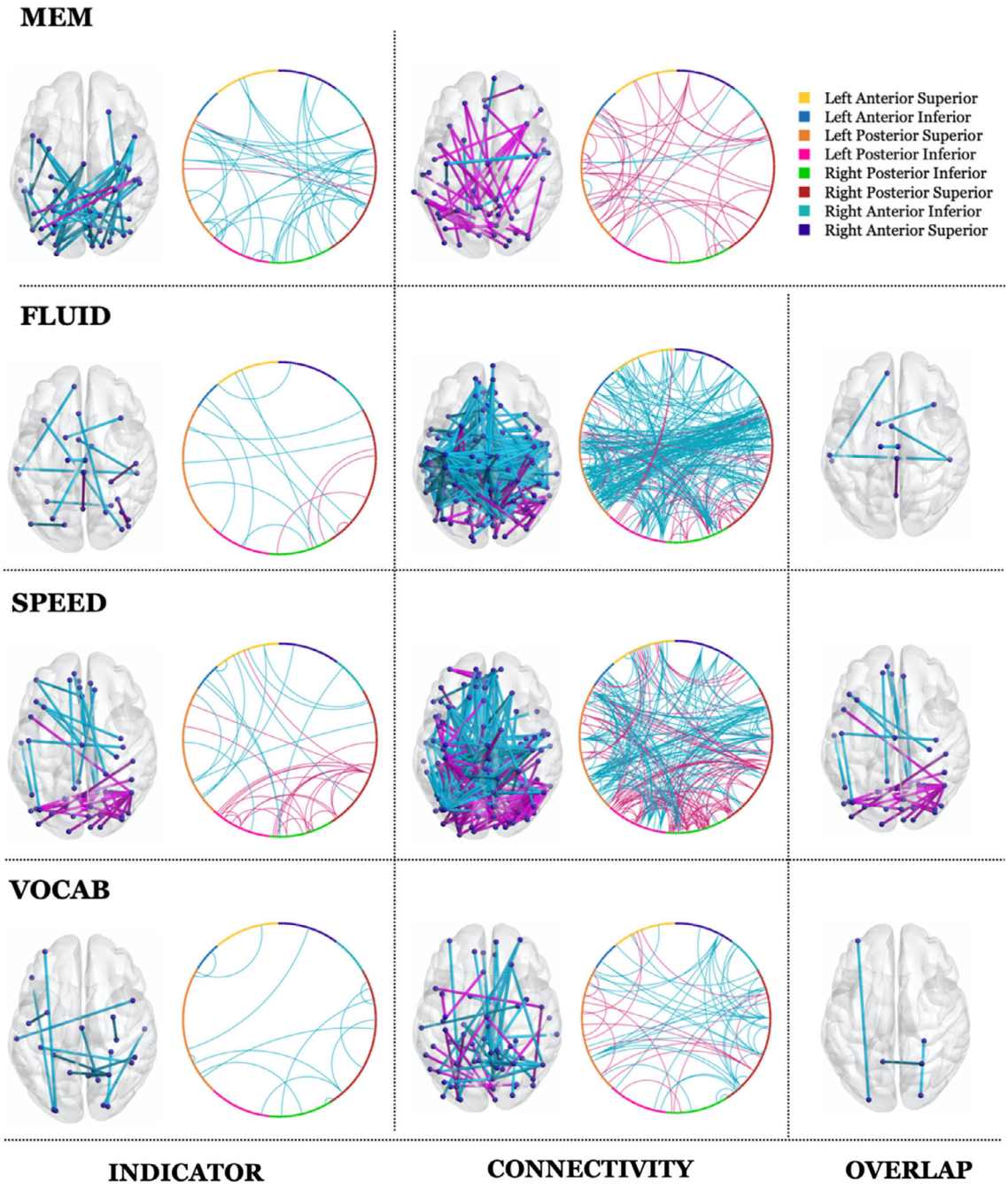

FIGURE 2 Edges demonstrating a significant age effect on (a) indicator correlation values (e.g., domain-selectivity); (b) strength of functional connectivity from the regression models, and (c) the overlap between models. As a reminder, linear regression analysis was performed only on RA-selective edges emerging from the one-way *t* tests across participants. Presented to the left of each subpanel are axial slices of significant edges, where negative correlations are presented in blue and positive correlations are presented in pink. Presented to the right of each subpanel are circular plots reflecting the topological organization of the brain divided into octants along the three coordinate planes (Anterior–Posterior, Superior–Inferior, Right–Left). The color of the nodes represents the octant to which the node belongs. The order of nodes within each octant was decided based on Euclidean distance from the common center point (0, 0, 0)

whereas the FLUID domain presented few edges displaying an age-effect on domain-selectivity, instead it presented the highest number of edges displaying a significant relationship between behavior and domain-selectivity. Notably, contrary to the SPEED domain, two edges displayed a significant positive relationship between both age and behavior and domain-selectivity, meaning that domain-selectivity increased as both age and behavioral performance increased. These edges connected the right inferior and medial occipital cortex to the right angular gyrus. The right medial occipital cortex also displayed high connectivity to the left precentral gyrus.

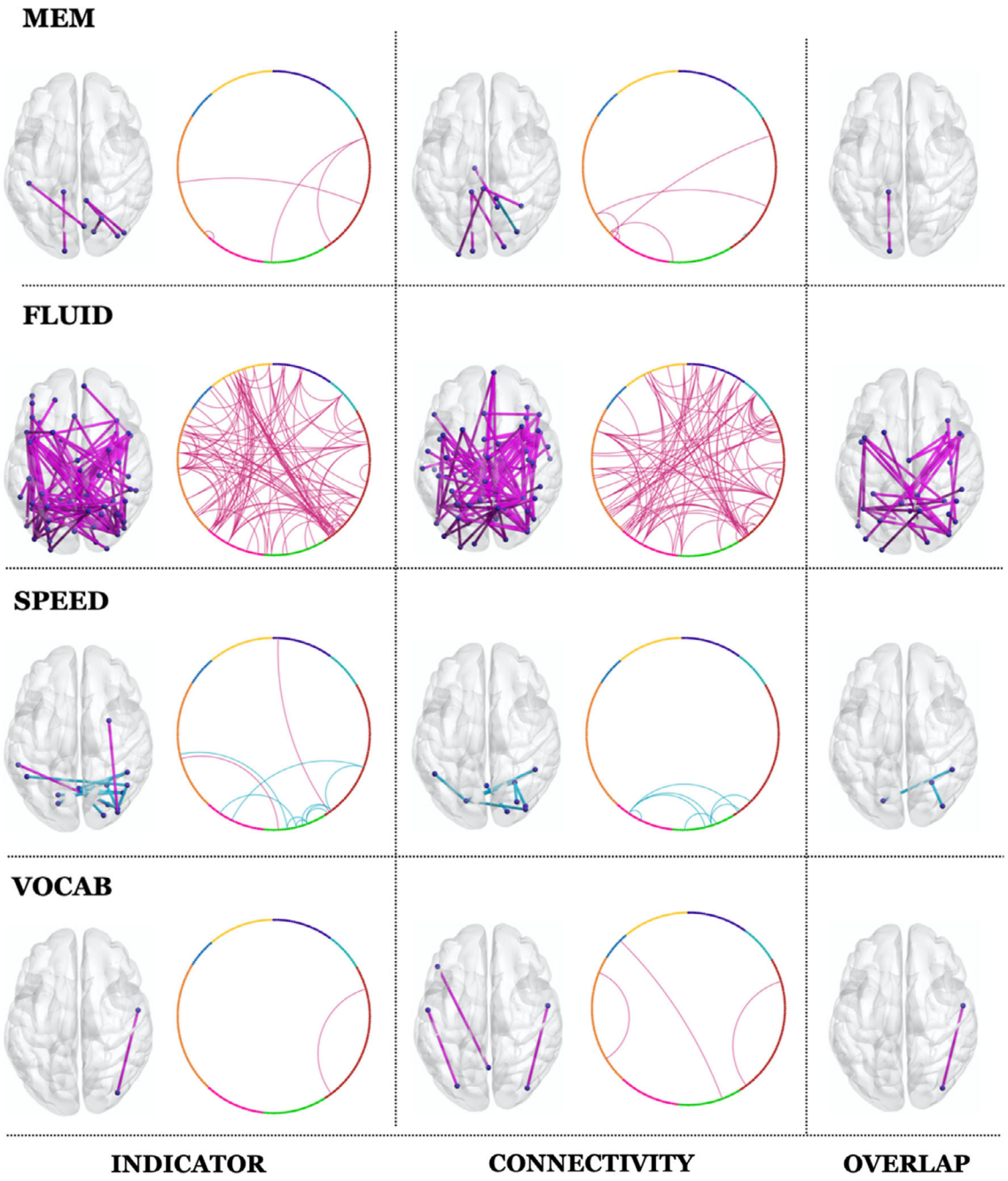

FIGURE 3 Edges demonstrating a significant behavior effect on (a) indicator correlation values (e.g., domain-selectivity); (b) strength of functional connectivity from the regression models, and (c) the overlap between models. As a reminder, linear regression analysis was performed only on RA-selective edges emerging from the one-way *t* tests across participants. Presented to the left of each subpanel are axial slices of significant edges, where negative correlations are presented in blue and positive correlations are presented in pink. Presented to the right of each subpanel are circular plots reflecting the topological organization of the brain divided into octants along the three coordinate planes (Anterior–Posterior, Superior–Inferior, Right–Left). The color of the nodes represents the octant to which the node belongs. The order of nodes within each octant was decided based on Euclidean distance from the common center point (0, 0, 0)

Interaction

A few edges displayed a significant moderating effect of Age on the relationship between domain-selectivity and Behavior (see left section of Figure 4). For the MEM domain, three edges displayed a negative interaction effect—that is, increasing age led to a decrease in behavioral performance with higher values of domain-selectivity. The FLUID and SPEED domains, on the other hand, each expressed one edge displaying a positive interaction effect, or a strengthening of the positive relationship between behavior and domain-selectivity with advancing age. Interestingly, edges displaying this positive interaction were long-range projections connecting medial frontal regions to more posterior cortical sites. The VOCAB domain contained the most

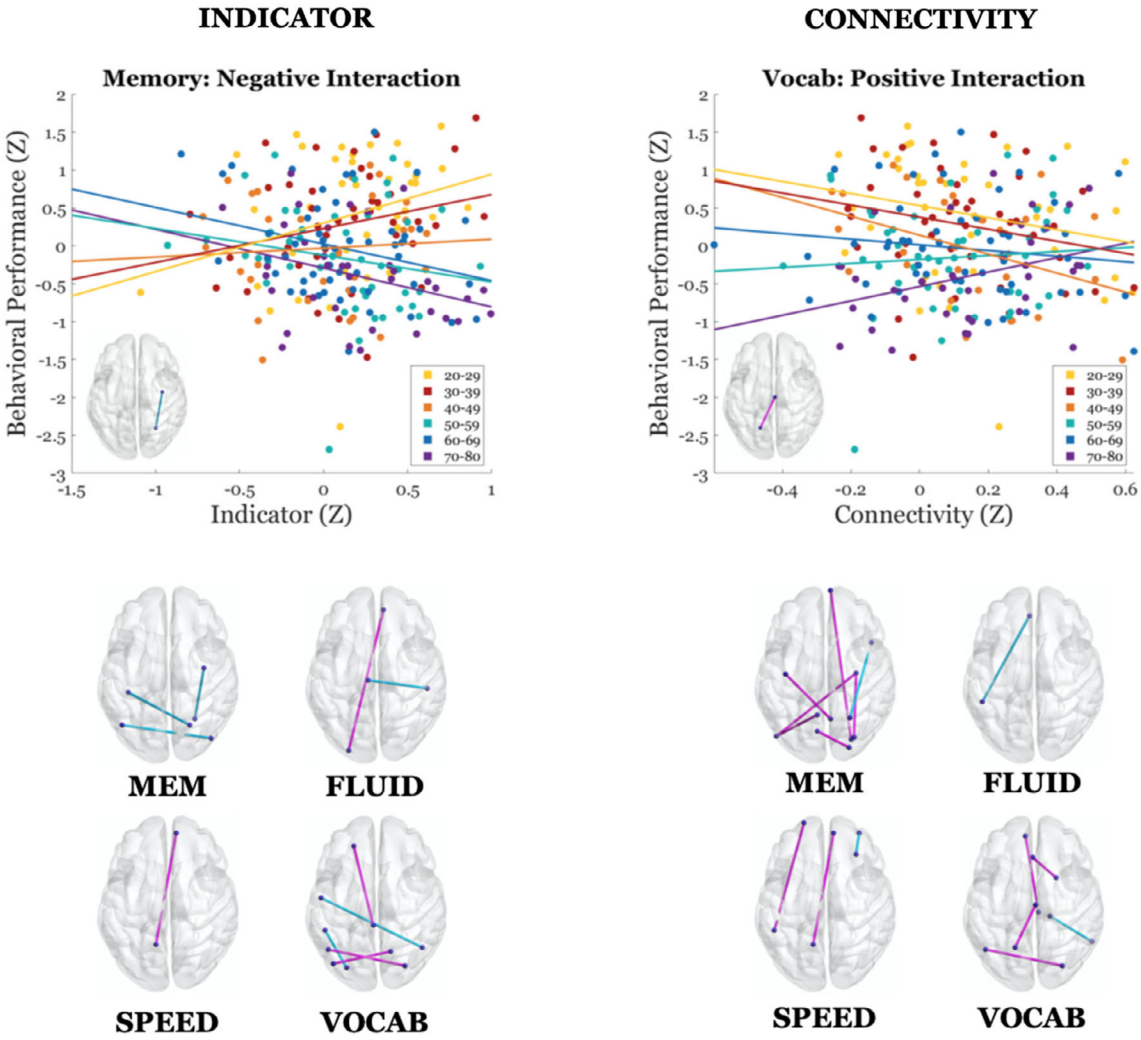

FIGURE 4 Edges demonstrating a significant Interaction effect between Age and Behavior for (a) indicator correlation values (e.g., domain-selectivity) and (b) strength of functional connectivity from the regression models. In the upper panel, graphs are presented reflecting the Age moderation effect in two sample edges (one for the indicator regression and one for the connectivity regression). In each graph, Behavioral Performance (Z-score) is presented on the y-axis and either indicator correlation (Z-transformed coefficient) or connectivity values (Z-transformed coefficient) on the x-axis. Age is stratified by decade and color coded, each dot representing a participant. The colored lines represent the least-squared fit. The bottom-left of each graph denotes the edge depicted in the graph. In the bottom panel, as previously stated, axial slices of significant edges are presented, where negative correlations are indicated in blue and positive correlations are indicated in pink

edges displaying a significant interaction in both directions. Of the edges displaying a positive interaction, two extended from medial occipital regions bilaterally to the medial temporal cortex and precuneus.

3.3.2 | Associations of connectivity regression

Age

Compared to the indicator regression analysis, functional connectivity values regressed on Age generally yielded many more edges displaying a significant relationship between the two, with the FLUID domain presenting the highest number (see right section of Figure 2). There was a clear concentration of bilateral negative connections between right and left posterior superior regions of the cortex, mainly linking the left post and paracentral lobule and medial cingulate to right parietal structures. Conversely, the MEM domain primarily displayed edges with a positive relationship between Age and connectivity diffuse across the brain. Both the FLUID and SPEED domains displayed edges with a positive relationship between Age and connectivity mainly in posterior regions of the cortex, with a higher concentration for the SPEED domain. Interestingly, several of these positive edges shared overlap with the significant edges from the indicator regression analysis, consistently in the positive direction- that is, as age increased, both domain-selectivity and functional connectivity increased. Furthermore, the node of the right superior posterior cortex (medial temporal lobe) that served as a connective "hub" in the indicator regression analysis was also present in

the overlap between models. A connective hub displaying a negative relationship between Age and connectivity strength was also observed in left inferior parietal lobule. Additionally, there were three long-range negative connections also present in the overlap linking the cerebellum to the bilateral medial orbitofrontal cortex and left anterior cingulate. The VOCAB domain displayed a right-lateralized reduction in connectivity with age, notably among long-range connections linking the superior frontal gyrus with the precuneus in addition to age-related increases in connectivity among left posterior superior regions.

Behavior

Few edges displayed a significant relationship between behavior and functional connectivity across domains except for the FLUID domain (see right panel of Figure 3). For the FLUID domain, all significant edges displayed a positive relationship between behavior and functional connectivity. Additionally, six of these edges also displayed a positive relationship between age and connectivity, indicating that connectivity increased with age and that behavior also increased with increasing strength of connectivity. Conversely, for the SPEED domain, only edges expressing a negative relationship between connectivity strength and behavioral performance were significant. Additionally, three of these edges, linking the cerebellum to visual cortical areas as well as the right medial occipital cortex to the right fusiform, the displayed increased connectivity with advancing age. The VOCAB domain displayed the fewest edges reflecting a relationship between behavior and connectivity strength; however, there was one edge, connecting the right medial occipital gyrus to the rolandic operculum, that still displayed an overlap between regression models, indicating that as both domain-selectivity and connectivity strength increased, behavior increased. Additionally, two left-hemispheric edges displayed the same positive relationship, namely connecting the inferior frontal gyrus to the vermis and the medial occipital gyrus to heschl's gyrus.

Interaction

For the MEM domain, contrary to the negative moderation effect of Age on the relationship between behavioral performance and domain-selectivity, age mainly exerted a positive effect on the relationship between behavior and connectivity strength in significant edges (see right section of Figure 4). These edges linked the right putamen and left precuneus to occipital lobe sites in addition to the cerebellum to medial orbitofrontal cortex. The VOCAB domain also displayed edges with a mainly positive moderation effect of Age on the relationship between Behavior and connectivity strength. These edges were inter-hemispheric and distributed along the posterior–anterior axis whereas the one negative interaction linked the right parahippocampal gyrus to the right inferior temporal lobe. For the SPEED domain, a positive moderation effect of Age was observed for two long-range connections between the left and right superior frontal lobule and left precuneus and medial temporal lobe. Interestingly, a negative moderation effect of Age was found between two regions of the right medial frontal cortex.

4 | DISCUSSION

The current study aimed to identify task-based functional networks pertaining to four cognitive domains (i.e., RAs), for which unique neural network activation patterns had been previously derived (Habeck et al., 2016; Habeck et al., 2018), and to investigate differences in both selectivity and connectivity of these networks as they relate to age and behavior. To this end, we report the functional connectivity results from 287 adults ranging from 20 to 80 years who performed 12 in-scanner behavioral tasks across our four RA domains. Exploiting an in-scanner fMRI multiple task testing design, we derived a set of domain-selective edges that emerged from the neural data across tasks pertaining to the same RA performing multiple one-way *t* tests across participants. We next used these domain-selective edges as an index to explore the effect of age, behavior, and the interaction term as an indicator of age moderation, on the both selectivity and connectivity. That is, for each edge, we created two linear regression models, regressing either selectivity or connectivity on age, behavior, and the interaction between the two. We then looked at the conjunction of significant edges between models for each predictor term. Overall, different subsets of edges emerged as displaying a significant relationship between our neural measures and age or behavioral performance for each of the four cognitive domains tested. Furthermore, the FLUID domain particularly stood out as vulnerable to the effects of age as well as displaying the most extensive connectivity and selectivity "footprint" for behavioral performance.

Results from the indicator variable correlation analysis identified edges that were attributable to each of our RA domains. Moreover, evaluation of how significant edges relevant to one domain behaved cross-domain revealed that strength of selectivity was indeed lower for all other domains, which was further expressed in the majority of participants. This confirms the domain-selective nature of these edges and reinforces the separability of these four domains of cognition that have previously been postulated in the literature (Salthouse & Ferrer-Caja, 2003).

For the speed domain, results from both the indicator and connectivity models revealed edges whose selectivity and connectivity strength increased with age, notably concentrated at posterior cortical sites. One node located in the right superior posterior cortex (middle temporal gyrus; BA37) served as a connective "hub." Previous studies have linked this region to conceptual action processing and action understanding (Kable, Kan, Wilson, Thompson-Schill, & Chatterjee, 2005; Simos et al., 2017). A negative connective "hub" between age and connectivity strength was also present in the left inferior parietal lobule, which is an area that has been implicated in visuospatial processing and multimodal representations, potentially serving visually guided action and navigation (Kravitz, Saleem, Baker, & Mishkin, 2011). Interestingly, despite the age-related increases in both domain-selectivity and connectivity strength, behavior significantly decreased in, notably, right posterior regions. Taken together, these findings could support accounts of age-related reductions in hemispheric lateralization that potentially points to inefficient bilateral recruitment of neural resources for tasks typically hemispherically

specialized, such as that of motor-related processing (Mutha, Haaland, & Sainburg, 2012). Additionally, the negative relationship between connectivity strength and age in long-range connections extending from anterior nodes could support previous findings of reduction in prefrontal and motor cortical coupling but enhanced local coupling within posterior motor and premotor cortices with advancing age (Rowe et al., 2006). This finding is somewhat at odds with theories positing an age-related anterior shift in processing that has been typically attributed to functional compensation (Davis et al., 2007). However, maintenance of long-range connectivity may be necessary to successful task performance among older adults, as a positive interaction effect was found for one long-range connection between the left superior medial frontal cortex and right precuneus.

For the memory domain, the effect of age on domain-selectivity resulted in edges principally expressing a reduction in domain-selectivity with increasing age whereas for connectivity, edges primarily expressed an increased in connectivity with age. Interestingly, this was the only domain that did not express overlap in edges expressing a significant effect of age on either domain-selectivity or connectivity. Despite the primarily negative effect of age on domain-selectivity, nodes connecting these negative edges were linked to a positive relationship between behavior and domain-selectivity, located in right posterior regions of the inferior/medial occipital cortex and cuneus. Edges where behavioral performance was positively related to connectivity strength were bilaterally located across the angular gyrus, medial cingulate, inferior/medial occipital cortex, thalamus, lingual gyrus, and precuneus. A largely positive interaction effect between age and behavior was also found in areas including the putamen, inferior/medial occipital cortex, medial temporal pole, and precuneus in addition to the cerebellum and medial orbitofrontal cortex. The involvement of posterior portions of the occipital cortex across model analyses could support previous findings of common engagement of these regions in both visual search and memory search tasks (Makino, Yokosawa, Takeda, & Kumada, 2004) as well as the reactivation of sensory regions in the recollection of visual memory (Wheeler, Petersen, & Buckner, 2000). Rather unsurprisingly, several structures additionally belonging or related to the limbic system were observed. For instance, the precuneus is a structure that has been widely implicated in episodic memory retrieval (for a review, see Cavanna & Trimble, 2006). The thalamus has also been linked to particular aspects of episodic memory function, including selection of stimuli for encoding and retrieval strategies (Van Der Werf, Jolles, Witter, & Uylings, 2003). These results jointly indicate a prominent role of the limbic system and structures possessing thalamcortical projections in maintaining the integrity of episodic memory across the lifespan. Despite the extensive findings displaying the consistent involvement of prefrontal cortical (PFC) regions in both episodic memory encoding and retrieval (for a review, see Tromp, Dufour, Lithfous, Pebayle, & Després, 2015), we only observed one connection displaying a positive interaction effect between age, behavior, and connectivity in the right orbitofrontal cortex. Right PFC activation has been observed during the retrieval phase of episodic information (Morcom, Good, Frackowiak, & Rugg, 2003; Tulving, Kapur, Craik, Moscovitch, & Houle, 1994). However, as we did not differentiate between encoding and retrieval phases among memory tasks, making informed speculation difficult.

The fluid domain displayed the highest number of significant edges emerging from the connectivity regression models, for both age and behavior. Perhaps the most salient finding was the vast bilateral connectivity between posterior superior regions of the cortex that were declining with age in addition to an age-related reduction in connectivity strength between frontal and parietal regions. Distributed fronto-parietal networks have been linked to reasoning ability (Wendelken, Ferrer, Whitaker, & Bunge, 2015), with the posterior parietal cortex playing an integral role (for a meta-analysis, see Wendelken, 2014). The current findings suggest a potential age-related decline in these networks. When analyzing the relationship between behavior and connectivity strength, only edges displaying a positive relationship emerged, with one node in the right frontal superior medial cortex, corresponding to Brodmann's area (BA) 10, linking frontal cortex to parietal regions. BA10 has been previously found to account for individual age-related differences in fluid intelligence (Kievit et al., 2014). Other prominent regions displaying a significant positive relationship between behavior and connectivity demonstrated bilateral crossover between parietal and occipital regions of the cortex. Within these regions, several edges additionally displayed an overlap in significance between age and behavior. Interestingly, these edges of overlap demonstrated a positive relationship between age, behavior, and connectivity strength, meaning that as connectivity strength increased, both age and behavior increased. These edges were primarily found in right-lateralized regions nonexhaustively including the angular gyrus, precuneus, insula, posterior cingulum, and medial occipital lobe. The presence of the posterior cingulum corroborates a previous finding from our lab in which preliminarily derived patterns of the fluid intelligence RA also revealed this region to be significant (Stern et al., 2014). Furthermore, the posterior cingulum has been found to be a hub for functional connections in the DMN, along with the precuneus and angular gyrus (Andrews-Hanna, Reidler, Sepulcre, Poulin, & Buckner, 2010). Previous literature has pointed to a greater left-lateralization of intelligence as formalized by the parieto-frontal integration theory of intelligence (Jung & Haier, 2007) and substantiated by studies of regional metabolic processing associated with fluid intelligence (Nikolaidis et al., 2016). We did observe a somewhat left-lateralization for negative age effects, with age-related decreases in connectivity in the left medial frontal cortex and anterior cingulate. One edge connecting the anterior cingulate to the medial temporal gyrus displayed a significant negative interaction between age and behavior on connectivity strength, meaning that behavior increased with increasing connectivity at younger ages but the inverse pattern was found with advancing age. The anterior cingulate cortex has been shown to be strongly engaged in working memory and tasks of high attentional demand (Lenartowicz & McIntosh, 2005). Given the cognitive complexity that is associated with fluid intelligence—a general mental ability comprising reasoning, problem solving, and learning—it indeed has been shown to share overlap with abilities such as working memory (see Salthouse, Pink, & Tucker-Drob, 2008)

and attempts have been made toward its functional parcellation into networks including attention, salience, and cognitive control (for a meta-analysis, see Santarnecchi, Emmendorfer, & Pascual-Leone,-2017). However, our finding of a more right-lateralized posterior network displaying increases between age, behavior, and connectivity presents a novel consideration for the functional network organization in the aging brain.

The vocabulary domain, on the other hand, demonstrated the lowest number of significant domain-selective edges in the indicator analysis. We observed an overall right-lateralized reduction in both domain-selectivity and connectivity strength with increasing age, particularly among long-range connections linking the superior frontal gyrus with the precuneus. One hypothesis could be that, given an arguably left-lateralized language network (Dronkers, Wilkins, Van Valin Jr, Redfern, & Jaeger, 2004) combined with the fact that vocabulary is the one domain where older adults outperform younger adults (Salthouse & Davis, 2006; see Hartshorne & Germine, 2015), an increase in left-hemispheric connectivity could suggest a strengthening of specialized networks, rather than compensation of processing. However, when looking at the relationship between behavior and connectivity, the edge that displayed a positive relationship between behavior and both domain-selectivity and connectivity strength linked the right rolandic operculum to the right middle occipital gyrus. Both the rolandic operculum and the middle occipital gyrus have been implicated in language and speech production (Nakamichi et al., 2018) and visual word form processing (Levy et al., 2008), respectively, although in the left hemisphere. Focusing only on edges displaying increases between behavior and connectivity strength, we observed significant behavior-related connectivity between the inferior frontal gyrus and vermis. The inferior frontal gyrus is a well-studied integral region to language production (Tyler et al., 2011). Additionally, more recent research on cerebellar functions has argued for a modulatory role in non-motor language processes such as lexical retrieval and other language dynamics (Marien, Engelborghs, Fabbro, & De Deyn, 2001). Interesting, the majority of edges displaying a positive interaction between age, behavior, and connectivity strength were bilateral connections linking the left anterior cingulate to right subcortical structures (i.e., putamen and thalamus), the left middle temporal gyrus to the right middle occipital gyrus, and the left superior parietal gyrus to the right supplementary motor cortex. Activations of regions outside of canonical language processing could be due to recruitment of what has been termed "domain-general" language systems, which includes regions typically linked to functions such as cognitive control and memory (Campbell & Tyler, 2018; Fedorenko, 2014). Indeed, we witnessed a significant interaction extending from the anterior cingulate to subcortical structures, which could evidence the engagement of such cognitive control mechanisms.

The motivation of the RANN study was to define patterns of activation associated with four latent abilities, or RA, that had repeatedly been identified as comprising the majority of age-related cognitive changes (Salthouse, 2005, Salthouse, 2009b). To this end, our lab had previously derived neural patterns based on voxel activations that demonstrated age-invariance across the lifespan (Habeck et al., 2016). In the current study, we aimed to investigate functional connectivity networks associated with each RANN domain and to analyze the change in both selectivity and connectivity strength among each ability as a function of age and behavioral performance. We found that different network organizations accompany different RAs and that, despite age-invariant patterns being derived at the voxel level, some of these edges are prone to significant change in both domain-selectivity and connectivity strength with advancing age. Additionally, some edges expressed significant changes between connectivity and behavioral performance, rendering different configurations by domains.

Given the richness of data presented herein, there are several further considerations that could be made in attempting to capture age-related changes in cognition. These additional analyses went beyond the current scope of the paper and remain for the future. For instance, we could consider the overlap in edge selectivity that had emerged between different domains in the indicator analysis to see if there is any domain-general processing network that might then display significant modulation with age or differences in behavioral performance. Additionally, we could include education and NART as covariates in our regression models.

We employed Power et al.'s (2011) parcellation scheme, which divides the brain based on 14 functional networks, and we could have investigated how these networks could have differentially interacted in representing domain-selectivity across our RAs and how age could have impacted network configuration on a variety of graph theoretical metrics such as network integration/segregation, modularity, global/local efficiency, etc. Several recent studies have pointed to age-related differences in network metrics (for a review, see Chan, Park, Savalia, Petersen, & Wig, 2014; Damoiseaux, 2017; Geerligs, Renken, Saliasi, Maurits, & Lorist, 2014; Shaw, Schultz, Sperling, & Hedden, 2015). One potential limiting factor is the use of a parcellation scheme that has been derived in younger adults, which assumes consistency in spatial organization across the life span. Recent work has challenged this notion, arguing that age-dependent changes in macro-anatomy introduce greater variability that may compromise anatomical alignment in older adults; thus, alternative parcellation schemes have been proposed (see Han et al., 2018). Given the remaining questions about the validity and persistence across the lifespan, we confined the majority of our analyses to reporting edges and their constituent nodes, rather than omnibus measures whose derivation depends on Power's network taxonomy.

Taken together, our findings indicate that different functional connectivity patterns are associated with each of our RANN domains and that, at least at the level of functional associations between regions, the degree of selectivity and connectivity strength of some of these edges vary as a function of age and behavioral performance. Furthermore, our findings do not support an exclusively greater recruitment of frontal regions as has been posited by theories supporting anterior shifts in activation increases with advancing age. We acknowledge that findings from voxel-based activation data do not necessarily extend to higher-order moments such as functional connectivity outcomes, despite a naturally tendency toward forging

this relationship. However, in showing an overall more posterior involvement of regions displaying increases in domain-selectivity and connectivity strength with age, our results do argue for a more prominent role of posterior regions in the aging process, at least in terms of network dynamics. Interestingly, though, recent accounts have disputed anterior-shift accounts, claiming that greater activation in PFC in older adults carries less information than visual region activation, for example, speaking against the notion of PFC compensation (Morcom & Henson, 2018). Future studies that directly test these hypotheses are critical to advancing more refined theories of aging.

ACKNOWLEDGMENTS

We wish to gratefully acknowledge support from the grant NIH/NIA R01AG038465-06.

CONFLICT OF INTERESTS

The authors confirm that they have no conflict of interest to declare.

DATA AVAILABILITY STATEMENT

The data that support the findings of this study are available from the corresponding author upon reasonable request.

ORCID

Georgette Argiris https://orcid.org/0000-0003-0999-2926
Christian Habeck https://orcid.org/0000-0001-9961-7446

REFERENCES

Addis, D. R., Leclerc, C. M., Muscatell, K. A., & Kensinger, E. A. (2010). There are age-related changes in neural connectivity during the encoding of positive, but not negative, information. *Cortex*, *46*, 425–433.

Aiken, L. S., & West, S. G. (1991). *Multiple regression: Testing and interpreting interactions*. Newbury Park, CA: Sage Publications.

Andrews-Hanna, J. R., Reidler, J. S., Sepulcre, J., Poulin, R., & Buckner, R. L. (2010). Functional-anatomic fractionation of the brain's default network. *Neuron*, *65*(4), 550–562.

Benjamini, Y., & Yekutieli, D. (2001). The control of the false discovery rate in multiple testing under dependency. *The Annals of Statistics*, *29*(4), 1165–1188.

Birn, R. M., Diamond, J. B., Smith, M. A., & Bandettini, P. A. (2006). Separating respiratory-variation-related fluctuations from neuronal-activity-related fluctuations in fMRI. *NeuroImage*, *31*(4), 1536–1548.

Campbell, K. L., & Tyler, L. K. (2018). Language-related domain-specific and domain-general systems in the human brain. *Current Opinion in Behavioral Sciences*, *21*, 132–137.

Carp, J. (2013). Optimizing the order of operations for movement scrubbing: Comment on Power et al. *NeuroImage*, *76*, 436–438.

Cavanna, A. E., & Trimble, M. R. (2006). The precuneus: A review of its functional anatomy and behavioural correlates. *Brain*, *129*(3), 564–583.

Chan, M. Y., Park, D. C., Savalia, N. K., Petersen, S. E., & Wig, G. S. (2014). Decreased segregation of brain systems across the healthy adult lifespan. *Proceedings of the National Academy of Sciences*, *111*(46), E4997–E5006.

Dale, A. M., Fischl, B., & Sereno, M. I. (1999). Cortical surface-based analysis: I. *Segmentation and Surface Reconstruction. Neuroimage*, *9*(2), 179–194.

Damoiseaux, J. S. (2017). Effects of aging on functional and structural brain connectivity. *NeuroImage*, *160*, 32–40.

Damoiseaux, J. S., Beckmann, C. F., Arigita, E. J. S., Barkhof, F., Scheltens, P., Stam, C. J., … Rombouts, S. A. R. B. (2008). Reduced resting-state brain activity in the "default network" in normal aging. *Cerebral Cortex*, *18*, 1856–1864.

Davis, S. W., Dennis, N. A., Daselaar, S. M., Fleck, M. S., & Cabeza, R. (2007). Que PASA? The posterior–anterior shift in aging. *Cerebral Cortex*, *18*(5), 1201–1209.

Dennis, N. A., Hayes, S. M., Prince, S. E., Madden, D. J., Huettel, S. A., & Cabeza, R. (2008). Effects of aging on the neural correlates of successful item and source memory encoding. *Journal of Experimental Psychology. Learning, Memory, and Cognition*, *34*, 791–808.

Dronkers, N. F., Wilkins, D. P., Van Valin, R. D., Jr., Redfern, B. B., & Jaeger, J. J. (2004). Lesion analysis of the brain areas involved in language comprehension. *Cognition*, *92*(1–2), 145–177.

Ekstrom, R. B., Dermen, D., & Harman, H. H. (1976). *Manual for kit of factor-referenced cognitive tests* (Vol. 102). Princeton, NJ: Educational testing service.

Fedorenko, E. (2014). The role of domain-general cognitive control in language comprehension. *Frontiers in Psychology*, *5*, 335.

Geerligs, L., Renken, R. J., Saliasi, E., Maurits, N. M., & Lorist, M. M. (2014). A brain-wide study of age-related changes in functional connectivity. *Cerebral Cortex*, *25*(7), 1987–1999.

Habeck, C., Eich, T., Razlighi, R., Gazes, Y., & Stern, Y. (2018). Reference ability neural networks and behavioral performance across the adult life span. *NeuroImage*, *172*, 51–63.

Habeck, C., Gazes, Y., Razlighi, Q., Steffener, J., Brickman, A., Barulli, D., … Stern, Y. (2016). The reference ability neural network study: Life-time stability of reference-ability neural networks derived from task maps of young adults. *NeuroImage*, *125*, 693–704.

Han, L., Savalia, N. K., Chan, M. Y., Agres, P. F., Nair, A. S., & Wig, G. S. (2018). Functional parcellation of the cerebral cortex across the human adult lifespan. *Cerebral Cortex*, *28*(12), 4403–4423.

Hartshorne, J. K., & Germine, L. T. (2015). When does cognitive functioning peak? The asynchronous rise and fall of different cognitive abilities across the life span. *Psychological Science*, *26*(4), 433–443.

Jenkinson, M., Bannister, P., Brady, M., & Smith, S. (2002). Improved optimization for the robust and accurate linear registration and motion correction of brain images. *NeuroImage*, *17*(2), 825–841.

Jenkinson, M., & Smith, S. (2001). A global optimisation method for robust affine registration of brain images. *Medical Image Analysis*, *5*(2), 143–156.

Jung, R. E., & Haier, R. J. (2007). The Parieto-frontal integration theory (P-FIT) of intelligence: Converging neuroimaging evidence. *Behavioral and Brain Sciences*, *30*(2), 135–154.

Kable, J. W., Kan, I. P., Wilson, A., Thompson-Schill, S. L., & Chatterjee, A. (2005). Conceptual representations of action in the lateral temporal cortex. *Journal of Cognitive Neuroscience*, *17*(12), 1855–1870.

Kievit, R. A., Davis, S. W., Mitchell, D. J., Taylor, J. R., Duncan, J., Tyler, L. K., … Dalgleish, T. (2014). Distinct aspects of frontal lobe structure mediate age-related differences in fluid intelligence and multitasking. *Nature Communications*, *5*, 5658.

Kravitz, D. J., Saleem, K. S., Baker, C. I., & Mishkin, M. (2011). A new neural framework for visuospatial processing. *Nature Reviews Neuroscience*, *12*(4), 217–230.

Lenartowicz, A., & McIntosh, A. R. (2005). The role of anterior cingulate cortex in working memory is shaped by functional connectivity. *Journal of Cognitive Neuroscience*, *17*(7), 1026–1042.

Levy, J., Pernet, C., Treserras, S., Boulanouar, K., Berry, I., Aubry, F., … Celsis, P. (2008). Piecemeal recruitment of left-lateralized brain areas during reading: A spatio-functional account. *NeuroImage*, *43*(3), 581–591.

Liem, F., Geerligs, L., Damoiseaux, J. S., & Margulies, D. S. (2019). Functional connectivity in aging. In K. W. Schaie & S. Willis (Eds.), *Handbook of the psychology of aging* (9th ed.). San Diego: Academic Press.

Mak, L. E., Minuzzi, L., MacQueen, G., Hall, G., Kennedy, S. H., & Milev, R. (2017). The default mode network in healthy individuals: A systematic review and meta-analysis. *Brain Connectivity*, *7*(1), 25–33.

Makino, Y., Yokosawa, K., Takeda, Y., & Kumada, T. (2004). Visual search and memory search engage extensive overlapping cerebral cortices: An fMRI study. *NeuroImage*, *23*(2), 525–533.

Marien, P., Engelborghs, S., Fabbro, F., & De Deyn, P. P. (2001). The lateralized linguistic cerebellum: A review and a new hypothesis. *Brain and Language*, *79*(3), 580–600.

Mattis, S. (1988). *Dementia rating scale: DRS: Professional manual*. Odessa, Ukraine: Psychological Assessment Resources.

Morcom, A. M., Good, C. D., Frackowiak, R. S., & Rugg, M. D. (2003). Age effects on the neural correlates of successful memory encoding. *Brain*, *126*(1), 213–229.

Morcom, A. M., & Henson, R. N. (2018). Increased prefrontal activity with aging reflects nonspecific neural responses rather than compensation. *Journal of Neuroscience*, *38*(33), 7303–7313.

Mutha, P. K., Haaland, K. Y., & Sainburg, R. L. (2012). The effects of brain lateralization on motor control and adaptation. *Journal of Motor Behavior*, *44*(6), 455–469.

Nakamichi, N., Takamoto, K., Nishimaru, H., Fujiwara, K., Takamura, Y., Matsumoto, J., … Nishijo, H. (2018). Cerebral hemodynamics in speech-related cortical areas: Articulation learning involves the inferior frontal gyrus, ventral sensory-motor cortex, and parietal-temporal sylvian area. *Frontiers in Neurology*, *9*, 939.

Nikolaidis, A., Baniqued, P. L., Kranz, M. B., Scavuzzo, C. J., Barbey, A. K., Kramer, A. F., & Larsen, R. J. (2016). Multivariate associations of fluid intelligence and NAA. *Cerebral Cortex*, *27*(4), 2607–2616.

Onoda, K., Ishihara, M., & Yamaguchi, S. (2012). Decreased functional connectivity by aging is associated with cognitive decline. *Journal of Cognitive Neuroscience*, *24*, 2186–2198.

Power, J. D., Barnes, K. A., Snyder, A. Z., Schlaggar, B. L., & Petersen, S. E. (2012). Spurious but systematic correlations in functional connectivity MRI networks arise from subject motion. *NeuroImage*, *59*(3), 2142–2154.

Power, J. D., Cohen, A. L., Nelson, S. M., Wig, G. S., Barnes, K. A., Church, J. A., … Petersen, S. E. (2011). Functional network organization of the human brain. *Neuron*, *72*(4), 665–678.

Raven, J. C., Psychological Corporation, & H. K. Lewis (1962). Coloured progressive matrices. New York, NY: The Psychological Corporation.

Razlighi, Q. R., Habeck, C., Steffener, J., Gazes, Y., Zahodne, L. B., MacKay-Brandt, A., & Stern, Y. (2014). Unilateral disruptions in the default network with aging in native space. *Brain and Behavior: A Cognitive Neuroscience Perspective*, *4*(2), 143–157.

Rowe, J. B., Siebner, H., Filipovic, S. R., Cordivari, C., Gerschlager, W., Rothwell, J., & Frackowiak, R. (2006). Aging is associated with contrasting changes in local and distant cortical connectivity in the human motor system. *NeuroImage*, *32*(2), 747–760.

Sala-Llonch, R., Bartrés-Faz, D., & Junqué, C. (2015). Reorganization of brain networks in aging: A review of functional connectivity studies. *Frontiers in Psychology*, *6*, 663.

Sala-Llonch, R., Junqué, C., Arenaza-Urquijo, E. M., Vidal-Piñeiro, D., Valls-Pedret, C., Palacios, E. M., … Bartrés-Faz, D. (2014). Changes in whole-brain functional networks and memory performance in aging. *Neurobiology of Aging*, *35*, 2193–2202.

Salthouse, T. A. (1998). Independence of age-related influences on cognitive abilities across the life span. *Developmental Psychology*, *34*(5), 851–864.

Salthouse, T. A. (2005). Relations between cognitive abilities and measures of executive functioning. *Neuropsychology*, *19*(4), 532.

Salthouse, T. A. (2009a). When does age-related cognitive decline begin? *Neurobiology of Aging*, *30*(4), 507–514.

Salthouse, T. A. (2009b). Decomposing age correlations on neuropsychological and cognitive variables. *Journal of the International Neuropsychological Society*, *15*(5), 650–661.

Salthouse, T. A., & Babcock, R. L. (1991). Decomposing adult age differences in working memory. *Developmental Psychology*, *27*(5), 763–776.

Salthouse, T. A., & Davis, H. P. (2006). Organization of cognitive abilities and neuropsychological variables across the lifespan. *Developmental Review*, *26*, 31–54.

Salthouse, T. A., & Ferrer-Caja, E. (2003). What needs to be explained to account for age-related effects on multiple cognitive variables? *Psychology and Aging*, *18*(1), 91–110.

Salthouse, T. A., & Kersten, A. W. (1993). Decomposing adult age differences in symbol arithmetic. *Memory & Cognition*, *21*(5), 699–710.

Salthouse, T. A., Pink, J. E., & Tucker-Drob, E. M. (2008). Contextual analysis of fluid intelligence. *Intelligence*, *36*(5), 464–486.

Santarnecchi, E., Emmendorfer, A., & Pascual-Leone, A. (2017). Dissecting the parieto-frontal correlates of fluid intelligence: A comprehensive ALE meta-analysis study. *Intelligence*, *63*, 9–28.

Shaw, E. E., Schultz, A. P., Sperling, R. A., & Hedden, T. (2015). Functional connectivity in multiple cortical networks is associated with performance across cognitive domains in older adults. *Brain Connectivity*, *5*(8), 505–516.

Simos, P. G., Kavroulakis, E., Maris, T., Papadaki, E., Boursianis, T., Kalaitzakis, G., & Savaki, H. E. (2017). Neural foundations of overt and covert actions. *NeuroImage*, *152*, 482–496.

Stern, Y., Habeck, C., Steffener, J., Barulli, D., Gazes, Y., Razlighi, Q., … Salthouse, T. (2014). The reference ability neural network study: Motivation, design, and initial feasibility analyses. *NeuroImage*, *103*, 139–151.

Tromp, D., Dufour, A., Lithfous, S., Pebayle, T., & Després, O. (2015). Episodic memory in normal aging and Alzheimer disease: Insights from imaging and behavioral studies. *Ageing Research Reviews*, *24*, 232–262.

Tulving, E., Kapur, S., Craik, F. I., Moscovitch, M., & Houle, S. (1994). Hemispheric encoding/retrieval asymmetry in episodic memory: Positron emission tomography findings. *Proceedings of the National Academy of Sciences*, *91*(6), 2016–2020.

Tyler, L. K., Marslen-Wilson, W. D., Randall, B., Wright, P., Devereux, B. J., Zhuang, J., & Stamatakis, E. A. (2011). Left inferior frontal cortex and syntax: function, structure and behaviour in patients with left hemisphere damage. *Brain*, *134*(2), 415–431.

Van Der Werf, Y. D., Jolles, J., Witter, M. P., & Uylings, H. B. (2003). Contributions of thalamic nuclei to declarative memory functioning. *Cortex*, *39*(4–5), 1047–1062.

Wendelken, C. (2014). Meta-analysis: How does posterior parietal cortex contribute to reasoning? *Frontiers in Human Neuroscience*, *8*, 1042.

Wendelken, C., Ferrer, E., Whitaker, K. J., & Bunge, S. A. (2015). Fronto-parietal network reconfiguration supports the development of reasoning ability. *Cerebral Cortex*, *26*(5), 2178–2190.

Wheeler, M. E., Petersen, S. E., & Buckner, R. L. (2000). Memory's echo: Vivid remembering reactivates sensory-specific cortex. *Proceedings of the National Academy of Sciences*, *97*(20), 11125–11129.

Woodcock, R. W. (1989). *Woodcock-Johnson psycho-educational battery-revised (WJ-R)*. Allen, TX: Developmental Learning Materials.

Xia, M., Wang, J., & He, Y. (2013). *BrainNet Viewer*: A network visualization tool for human brain Connectomics. *PLoS One*, *8*(7), e68910.

SUPPORTING INFORMATION

Additional supporting information may be found online in the Supporting Information section at the end of this article.

How to cite this article: Argiris G, Stern Y, Habeck C. Reference Ability Neural Network-selective functional connectivity across the lifespan. *Hum Brain Mapp*. 2021;42: 644–659. https://doi.org/10.1002/hbm.25250